Am J Transl Res 2014;6(3):179-187
www.ajtr.org /ISSN:1943-8141/AJTR1401006

*Review Article*

# In vivo optical imaging of cancer metastasis using multiphoton microscopy: a short review

Koji Tanaka[1], Yuji Toiyama[1], Yoshinaga Okugawa[1], Masato Okigami[1], Yasuhiro Inoue[1], Keiichi Uchida[1], Toshimitsu Araki[1], Yasuhiko Mohri[1], Akira Mizoguchi[2], Masato Kusunoki[1]

*Departments of [1]Gastrointestinal and Pediatric Surgery, [2]Neural Regeneration and Cell Communication, Mie University Graduate School of Medicine, 2-174 Edobashi, Tsu, Mie 514-8507, Japan*

Received January 7, 2014; Accepted March 10, 2014; Epub May 15, 2014; Published May 30, 2014

**Abstract:** Intravital (in vivo) microscopy using fluorescently-tagged proteins is a valuable tool for imaging the expression of a specific protein, its subcellular location and the dynamics of specific cell populations in living animals. Recently, multiphoton microscopy including two-photon laser scanning microscopy (TPLSM) has been used in the field of tumor biology due to its ability to image target organs at higher magnification and at deeper depths from the tissue surface for longer time periods. We developed a method of *in vivo* real-time imaging for tumor metastasis using TPLSM with an organ stabilizing system, which allow us to observe not only a single tumor cell and its microenvironment for a long time, but also to observe the same organ of the same mouse at multiple time points in preclinical models. Here, we presented *in vivo* real-time images of 1) tumor cell arrest, 2) tumor cell-platelet interaction, 3) tumor cell-leukocyte interaction, and 4) metastatic colonization at the secondary organs as representative steps of metastatic process of experimental liver metastasis models using TPLSM.

**Keywords:** Cancer, metastasis, multiphoton microscopy

## Introduction

Cancer is a major health problem worldwide. More than 90% of cancer patients will die from metastatic disease. Therefore, translational metastasis research should be prompted urgently [1]. The underlying mechanism of tumor metastasis has being investigated using molecular biology techniques intensively. Despite of accumulating evidence of molecular biological mechanisms underlying tumor metastasis, our comprehensive understanding is still unsatisfactory [2].

Metastatic process consists of a number of steps: the detachment of tumor cells from the primary tumor mass, intravasation into blood or lymphatic vessels, escape or avoidance from the host immune system, survival in the bloodstream, arrest at the secondary distant organs, extravasation of the arrested tumor cells through vessels, and successful colonization of tumor cells in the surrounding microenvironment different from the primary tumor [3]. The underlying mechanism of each step has been examined by *in vitro* and/or *in vivo* studies.

Imaging of living animals at microscopic resolution (intravital microscopy, IVM) represents a powerful tool for understanding the dynamics of metastatic process in the natural microenvironment [4, 5]. The development of suitable mouse models is also important for intravital imaging of metastatic process.

The dorsal skinfold window chamber model remains to be used widely for IVM of invasion, intravasation, metastasis process, and tumor angiogenesis of implantable tumor [6]. This model also makes it possible to take multiple imaging sessions over several days and months. Since then, mammary window chamber model for orthotopic breast tumor [7] and cranial window chamber model for brain tumor [8] have been also developed.

## Intravital imaging of metastatic process using multiphoton microscopy

Multiphoton or two-photon laser scanning microscopy (TPLSM) utilizes two-photon excitation restricted to the focal plane by high-power, pulsed lasers. The longer-wavelengths as the

two-photon excitation source can penetrate deeper into tissues, up to 1000 μm [9]. The longer-(near-infrared) wavelengths can also reduce light scattering, resulting in an increased penetration depth. The two lower-energy excitation photons cause less photodamage, or phototoxicity (photobleaching). The absence of out-of-plane fluorescence can also contribute to the reduction of phototoxicity because of the two-photon excitation only at the focal plane [9]. TPLSM offers the above-mentioned numerous imaging benefits compared with single-photon confocal laser scanning microscopy (CLSM). Thus, TPLSM is thought to be an ideal tool for intravital imaging because of its ability to keep cell viability during imaging and to allow longer imaging time.

### In vivo imaging of murine liver metastasis model using TPLSM

*GFP-expressing mice*

Enhanced green fluorescent protein (EGFP)-transgenic C57/BL6-Tg (CAG-EGFP) mice were purchased from Japan SLC Inc. (Sizuoka, Japan). GFP-expressing nude mice (C57BL/6-BALB/c-nu/nu-EGFP) were purchased from AntiCancer Japan (Osaka, Japan).

GFP mice (20-22 g) were bred, housed in groups of six mice per cage and fed with a pelleted basal diet (CE-7, CLEA Japan Inc., Tokyo, Japan). Mice had free access to drinking water. They were kept in the animal house facilities at Mie University School of Medicine under standard conditions of humidity (50 ± 10%), temperature (23 ± 2°C) and light (12/12 h light/dark cycle), according to the Institutional Animal Care Guidelines. The experimental protocols were reviewed and approved by the Animal Care and Use Committee at Mie University Graduate School of Medicine.

*RFP-expressing cancer cell line*

RFP expressing murine (SL4) and human (HT-29) cancer cell lines were purchased from AntiCancer Japan (Osaka, Japan).

The inoculation of RFP-SL4 cells in GFP mice was used as a syngeneic tumor model. By contrast, the inoculation of RFP-HT29 cells in GFP nude mice was used as a xenogeneic tumor model.

Cancer cells were grown in monolayer cultures in RPMI 1640 (Sigma-Aldrich, Inc., St. Louis, MO. USA) supplemented with fetal bovine serum (FBS, 10% (v/v), GIBCO BRL, Tokyo, Japan), glutamine (2 mM), penicillin (100000 units/liter), streptomycin (100 mg/liter), and gentamycin (40 mg/liter) at 37°C in a 5% $CO_2$ environment. For routine passage, cultures were spilt 1:10 when they reached 90% confluence, generally every 3 days. Cells at the fifth to ninth passage were used for liver metastasis experiments, which were performed with exponential growing cells.

*Murine liver metastasis model*

RFP-expressing cancer cells were inoculated into the spleens of GFP mice, as a colorectal liver metastatic xenograft model [10]. RFP-HT29 or RFP-SL4 cancer cells at the fifth to ninth passage were harvested with trypsin/EDTA, and washed in serum-containing RPMI 1640 medium to inactivate any remaining trypsin. The cells were centrifuged and resuspended in phosphate-buffered saline (PBS). Finally, the cells were adjusted to $2\times10^7$ cells/mL for single cell suspensions.

GFP mice were anaesthetized using an anaesthetic mask with 4 L/min of isofluorane (4%; Forane, Abbott, Japan). Anaesthetic maintenance was achieved using 1.5-2% isoflurane and 4 L/min of $O_2$. Under direct vision, $2\times10^6$ cells were injected into the spleen using a 30-gauge needle through a small incision in the left lateral abdomen of anesthetized GFP mice.

### Liver stabilization for *in vivo* imaging using TPLSM

Previously we have reported a method of *in vivo* real-time imaging for various murine models using TPLSM with an organ stabilizing system, which allows high magnification (×600 or higher) and high resolution (at the cellular or subcellular level) images in living animals [11-17].

**Figure 1A** shows an overview of liver stabilization for in vivo imaging using TPLSM. The upper midline laparotomy was made (< 15 mm) in the anaesthetized mice. The left lateral lobe of the liver was identified and exteriorized through the laparotomy (**Figure 1B**). The liver lobe was then put onto a solder lug terminal with an instant adhesive agent (KO-10-p20, DAISO, Japan)

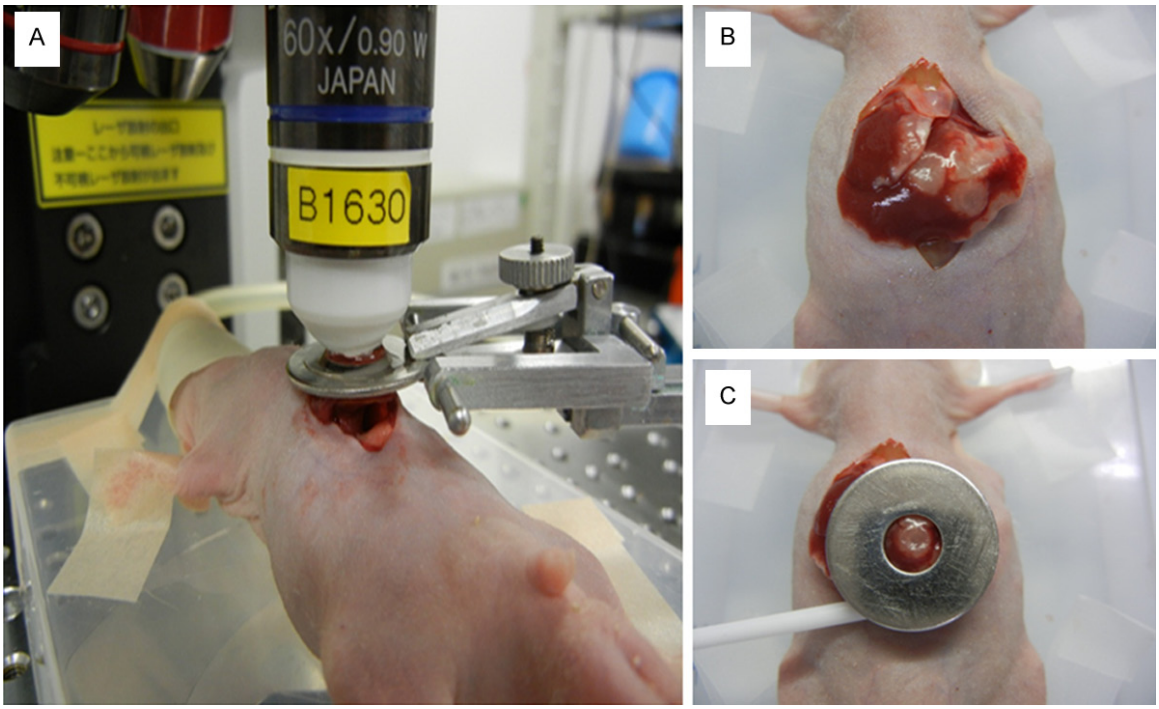


**Figure 1.** Overview of liver stabilization for *in vivo* imaging using TPLSM: A. Overview of liver stabilization using organ stabilizing system; B. Exteriorization of liver lobes; C. Liver stabilization using a solder lug terminal.

(**Figure 1C**). This organ stabilizer minimized the microvibration of the observed area caused by physiological heart beat and respiratory movements. After the application of PBS to the observed area, a thin cover glass was placed on the liver surface. After intravital TPLSM, a solder lug terminal was removed from the liver lobe using a release agent (KO-10-p8, DAISO, Japan). The liver surface were extensively washed by PBS to remove the residual release agent and blood coagulation mass. A sodium hyaluronate and carboxymethylcellulose membrane (Seprafilm Adhesion Barrier, Genzyme Corporation, Cambridge, MA) was placed between the liver and the abdominal wall to prevent postoperative dense adhesion. Body temperature was kept at 37°C throughout the experiments using a heating pad. Normal saline (200 μL) were administered intraperitoneally at 1-2 hour intervals for hydration during anesthesia.

### TPLSM setup

The detailed procedures for TPLSM setup were described as previously [14]. In brief, experiments were performed using an upright microscope (BX61WI; Olympus, Tokyo, Japan) and a FV1000-2P laser-scanning microscope system (FLUOVIEW FV1000MPE, Olympus, Tokyo, Japan). The use of special stage risers enabled the unit to have an exceptionally wide working distance. This permitted the stereotactically immobilized, anesthetized mouse to be placed on the microscope stage. The microscope was fitted with several lenses with high numeric apertures to provide the long working distances required for *in vivo* work, and with water-immersion optics. The excitation source in TPLSM mode was Mai Tai Ti: sapphire lasers (Spectra Physics, Mountain View, CA), tuned and mode-locked at 910 nm. The Mai Tai produces light pulses of about 100 fs width (repetition rate 80 MHz). Laser light reached the sample through the microscope objectives, connected to an upright microscope (BX61WI; Olympus, Tokyo, Japan). A mean laser power at the sample was between 10 and 40 mW, depending on the depth of imaging. Microscope objective lens were 4×UPlanSApo (numerical aperture of 0.16), 10×UPlanSApo (numerical aperture of 0.4), and 60×LUMPlanFI/IR (water dipping, numerical aperture of 0.9, working distance 2 mm), respectively. Data were analyzed using a FV10-ASW (Olympus, Tokyo, Japan). TPLSM images were acquired with 512×512 pixels

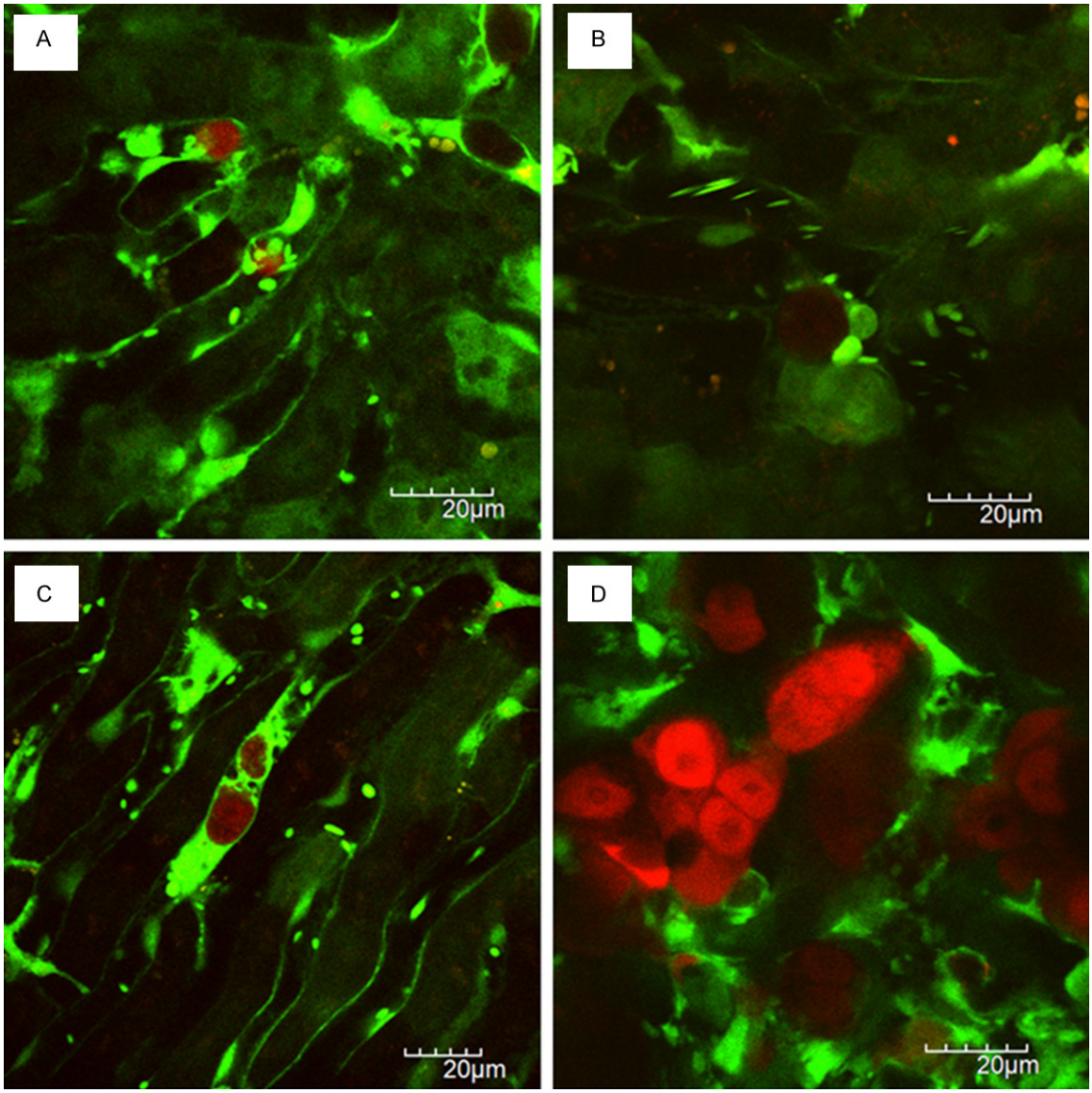


**Figure 2.** Visualization of liver metastatic process in xenogenic model: A. Tumor cell-platelet interaction; B. Tumor cell-leukocyte interaction; C. Platelets aggregation to the tumor cell; D. Liver metastatic colonization.

spatial resolution, from 210 μm field of view dimension, using a pixel dwelling time 4 μs. Two-photon fluorescence signals were collected by an internal detector (non-descanned detection method) at an excitation wavelength, to enable the simultaneous acquisition of EGFP signal and RFP (DsRed2) signal. Color-coded green and red images were imaged at the same time, and subsequently merged to produce single images.

### Imaging methods

The surface of the liver was screened at lower magnifications by setting out the X/Y plane and adjusting the Z axis manually to detect the optimal observation area containing RFP-expressing cancer cells (at least five areas). Subsequently, each area of interest was scanned at a higher magnification (water-immersion objective 60× with or without 2× zoom) by manually setting the X/Y plane and adjusting the Z axis either automatically or manually. The scanning areas were 200×200 μm (600×) or 100×100 μm (600× with 2× zoom) respectively. The imaging depth was determined arbitrarily. The laser power was adjusted according to the imaging depth. When imaging at larger depths, we increase the laser power level (up to near 100%) manually using laser power level

controller. To image the optimal simultaneous imaging of EGFP and RFP (DsRed2), detection sensitivity (brightness by HV) was adjusted manually for EGFP (450-500) or RFP (550-600), respectively.

### Visualization of liver metastatic process in xenogenic model (HT29)

Injection in the spleen or portal vein mimics hematogenous spread of tumor cells into the liver, which has been used by many researchers to create liver metastases. Tumor cells which were injected into the spleen circulated in the bloodstream (portal route), and then get stuck (or arrested) in the hepatic sinusoids. We can observe metastatic processes such as the tumor cell arrest, tumor endothelial interaction, tumor cell extravasation into the liver parenchyma, and the metastatic colonization in the liver using a liver metastasis model by intrasplenic injection of tumor cells.

### Tumor cell arrest

In our study, red-colored cancer cells were visualized in the green-colored liver structures of GFP mice at the single cell level (at a magnification of over 600×). Cancer cells were arrested in hepatic sinusoids 2 hours after injection. Circulating or rolling cancer cells in hepatic vessels were never observed during the 1 hour observation time. However, cancer cells appeared to gather into the central zone of hepatic lobes. It still remains unclear whether tumor cell arrest might be caused by molecular adhesion between cancer cells and hepatic endothelial cells or size-dependent occlusion.

### Tumor cell-platelet interaction

**Figure 2A** shows a tumor cell-platelet interaction within hepatic sinusoids. In GFP mice, red blood cells were not visualized [18]. Therefore, leukocytes were recognized as larger blood cells, and platelets were recognized as smaller ones within blood vessels. Within hepatic sinusoids, we observed that leukocytes including Kupffer cells were rolling or flowing *in vivo* real-time.

The fact that platelets are essential for hematogenous tumor metastasis has been demonstrated more than 4 decades ago and has been proven in a lot of experiments [19-21]. The interaction of tumor cells with platelets within the bloodstream occurs from the moment of tumor cell entry into the bloodstream (intravasation) to the moment that tumor cells leave from blood vessels (extravasation). Tumor cell induced platelet aggregation (TCIPA) is the phenomenon of which tumor cells can aggregate platelets. The advantageous role of TCIPA for tumor metastasis is thought to be the prolongation of tumor cell survival in the bloodstream and the protection of tumor cell by surrounding platelets from host immune system.

We observed in vivo real-time that platelets adhered to the intrasinusoidal (intravascular) tumor cells under normal blood flow, indicating a tumor cell-platelet interaction. **Figure 2C** also showed that platelets aggregated to the intrasinusoidal tumor cells like a protective coat. We think that it is thought to be a intravital imaging of TCIPA at high magnification and high resolution.

### Tumor cell-leukocyte interaction

**Figure 2B** shows a tumor cell-leukocyte interaction. The increase in neutrophil counts or neutrophil-to-lymphocyte ratios has demonstrated to be predictive value of poor prognosis or distant metastasis in several human malignancies [22, 23]. The presence of circulating tumor cells (CTC) has been shown to be a surrogate biomarker of hematogenous metastases [24, 25]. There is increasing evidence of CTC-neutrophil interaction in vitro. The role of neutrophils in CTC recruitment to the metastatic organs has been also reported [26, 27]. The interaction between tumor cells and neutrophils is thought to play an important role in tumor metastatic cascade.

We observed that leukocytes adhered to tumor cells within hepatic sinusoids *in vivo* real-time. We previously reported an intravital imaging of a leukocyte with ameboid morphology capturing a cancer cell [14]. The leukocyte with reticular protrusions is thought to phagocytose cancer cells in hepatic sinusoids. It remains unknown whether the interaction between neutrophils and intravascular tumor cells may be related to promote metastatic colonization by enhancing tumor cell extravasation following tumor cell-endothelial interaction or to suppress tumor metastasis by phagocytosing CTCs.

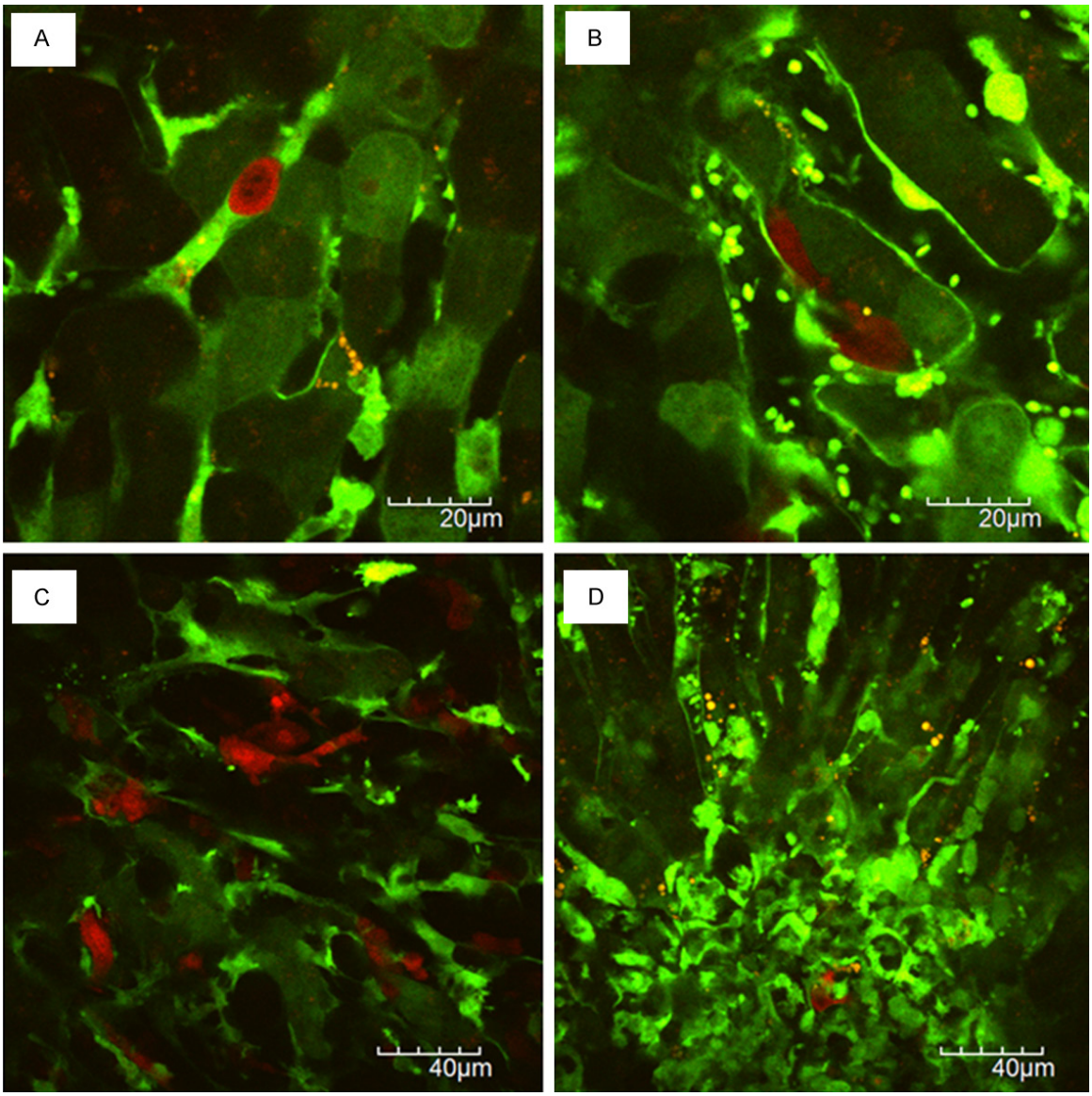


**Figure 3.** Visualization of liver metastatic process in syngeneic model: A. Tumor cell arrest; B. Tumor cell extravasation; C. Liver metastatic colonization showing diffuse growth pattern; D. Liver metastatic colonization with extensive stromal reaction.

### Metastatic colonization at the secondary organs

It has been the challenge for long time to image *in vivo* real-time the development of micrometastases at the secondary distant organs such as liver, lung, and brain using TPLSM because of motion artifact due to cardiac and respiratory movement.

We developed a method of *in vivo* real-time TPLSM imaging for experimental metastasis models using an organ stabilizing system, which allows to observe several steps of metastatic cascade at high magnification (×600 or higher) and high resolution (at the cellular or subcellular level) in living animals [14-17].

We also developed a method of time-series (at multiple time points) intravital TPLSM imaging in the same mice over the long experimental periods by the prevention of abdominal adhesions using a sodium hyaluronate and carboxymethylcellulose membrane (Seprafilm Adhesion Barrier, Genzyme Corporation, Cambridge, MA). Time-series intravital TPLSM imaging allow to

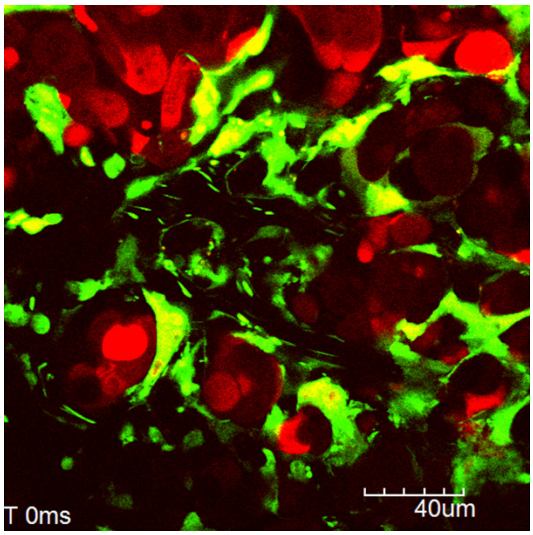


**Figure 4.** Tumor vessels of liver metastatic xenografts. Supplementary movie shows a time lapse imaging of a blood flow in the tumor vessels of liver metastatic xenografts.

image liver metastatic xenografts of the same mice until the formation of non-dissecting adhesions between the liver and the abdominal wall. We can take time-series images of liver metastatic xenografts in the same mice up to three time points.

**Figure 2D** shows a metastatic colonization of RFP-HT29 cells in the liver 2 month after the injection of tumor cells directly into the spleen. Liver metastases of RFP-HT29 showed multiple metastatic nodules macroscopically. Each metastatic nodule showed multiple micrometastatic clusters consisting of several tumor cells microscopically.

We couldn't observe the metastasis formation process continuously from a single tumor cell to micrometastatic colonization at the secondary organ because it is impossible to continue intravital TPLSM over 24 hours due to surgical stress by liver exteriorization. Therefore, it remains to be determined whether a single tumor cell retains as dormant state for long time or tumor cells directly proliferate within hepatic sinusoids (intravascular proliferation) or they proliferate in the liver parenchyma after the extravasation through hepatic endothelial cells [28].

### Visualization of liver metastatic process in syngeneic model (SL4)

Tumor transplantation models of metastasis require the inoculation of human (xenograft/xenogenic) or mouse (allograft/syngeneic) cells/tissue into murine hosts. Experimental metastasis models by either xenogenic or syngenic tumor involve the injection of tumor cells directly into the vascular system, which skip the formation of a primary tumor (orthotopically or ectopically) and the invasion into the local environment. Because murine tumor cells are inoculated into the immunocompetent hosts with the same species and genetic background, syngeneic tumor models provide a valuable preclinical tool of intact tumor-host interaction by intact immune systems in the metastatic cascade.

Similar to xenogenic tumor metastasis model using RFP-HT29, tumor cell arrest (**Figure 3A**), tumor cell-platelet interaction, tumor cell-leukocyte interaction, and metastatic colonization at the secondary organs (**Figure 3C**, **3D**) were observed *in vivo* real-time in syngeneic tumor metastasis model using RFP-SL4.

The space between hepatic endothelial cells and hepatocytes is named as the space of Disse (or perisinusoidal space). Spindle-shaped RFP-SL4 cells were localized in this space (**Figure 3B**). As shown in **Figure 3A**, RFP-SL4 cells are round-shaped just after intrasplenic injection. Thus, spindle-shaped RFP-SL4 cells were thought to be extravasated from hepatic sinusoids to the space of Disse 24 hours after injection.

However, we couldn't observe *in vivo* real-time the process of change in tumor cell morphology from a round-shape into a spindle-shape and the moment of intravascular tumor cells extravasate into liver parenchyma via vascular endothelium.

**Figure 2D** shows a metastatic colonization of RFP-HT29 cells in the liver 2 month after the injection of tumor cells directly into the spleen. Liver metastases of RFP-SL4 showed diffusely infiltrative growth macroscopically 14 days after the injection of tumor cells directly into the spleen. Microscopically, RFP-SL4 cells proliferated diffusely with extensive stromal reaction (**Figure 3C**, **3D**).

### Direct visualization of metastatic process at the secondary organs by TPLSM

Intravital TPLSM imaging using an organ stabilizing system can allow us to visualize each step

of metastatic cascade at high magnification and high resolution in living animals [14-17].

Time-series intravital TPLSM imaging can also allow us to visualize the same organ of the same animal at multiple time points (up to three times) during the long experimental periods. Therefore, we can directly visualize metastatic process at the secondary organs at high magnification and high resolution at least three times.

We presented *in vivo* real-time images of 1) tumor cell arrest, 2) tumor cell-platelet interaction, 3) tumor cell-leukocyte interaction, and 4) metastatic colonization at the secondary organs as representative steps of metastatic process of experimental liver metastasis models.

The spatiotemporal interactions between tumor cells and host cells during metastatic process can be visualized by using time-lapse and z-stacks imaging [14, 17]. **Figure 4** (supplementary movie 1) shows a blood flow in the tumor vessels of liver metastatic xenografts. As previously reported [15, 16], the interaction between intravascular tumor cells and endothelial cells or blood cells except for erythrocytes can be also observed. Platelet aggregation in tumor vessels and the adhesion of platelet aggregation to tumor endothelial cells were observed as the intravascular abnormalities within liver metastatic xenografts.

Although direct visualization of metastatic process at the secondary organs in vivo real-time might be valuable, there are still several issues which should be overcome. We must try to visualize the moment of each step of metastatic cascade at high magnification and high resolution in living animals. In our procedure, we couldn't observe the metastasis formation process continuously from a single tumor cell to micrometastatic colonization. We couldn't also observe the moment of change in tumor cell morphology or the moment of metastatic colonization by tumor cell division.

Direct visualization of metastatic process by real-time imaging for extended periods (over 24 hours per session) will help us to understand the spatiotemporal tumor-host interaction on tumor metastasis at the cellular and subcellular levels.

## Disclosure of conflict of interest

None.

**Address correspondence to:** Koji Tanaka, Department of Gastrointestinal and Pediatric Surgery, Mie University Graduate School of Medicine, 2-174 Edobashi, Tsu, Mie 514-8507, Japan. Tel: 81-59-231-5294; Fax: 81-59-232-6968; E-mail: qouji@clin.medic.mie-u.ac.jp

## References

[1] Sleeman J, Steeg PS. Cancer metastasis as a therapeutic target. Eur J Cancer 2010; 46: 1177-80.

[2] Valastyan S, Weinberg RA. Tumor metastasis: molecular insights and evolving paradigms. Cell 2011; 147: 275-92.

[3] Mathot L, Stenninger J. Behavior of seeds and soil in the mechanism of metastasis: a deeper understanding. Cancer Sci 2012; 103: 626-31.

[4] Pittet MJ, Weissleder R. Intravital imaging. Cell 2011; 147: 983-91.

[5] Beerling E, Ritsma L, Vrisekoop N, Derksen PW, van Rheenen J. Intravital microscopy: new insights into metastasis of tumors. J Cell Sci 2011; 124: 299-310.

[6] Hak S, Reitan NK, Haraldseth O, de Lange Davies C. Intravital microscopy in window chambers: a unique tool to study tumor angiogenesis and delivery of nanoparticles. Angiogenesis 2010; 13: 113-30.

[7] Kedrin D, Gligorijevic B, Wyckoff J, Verkhusha VV, Condeelis J, Segall JE, van Rheenen J. Intravital imaging of metastatic behavior through a mammary imaging window. Nat Methods 2008; 5: 1019-21.

[8] Kienast Y, von Baumgarten L, Fuhrmann M, Klinkert WE, Goldbrunner R, Herms J, Winkler F. Real-time imaging reveals the single steps of brain metastasis formation. Nat Med 2010; 16: 116-22.

[9] Ustione A, Piston DW. A simple introduction to multiphoton microscopy. J Microsc 2011; 243: 221-6.

[10] de Jong GM, Aarts F, Hendriks T, Boerman OC, Bleichrodt RP. Animal models for liver metastases of colorectal cancer: research review of preclinical studies in rodents. J Surg Res 2009; 154: 167-76.

[11] Toiyama Y, Mizoguchi A, Okugawa Y, Koike Y, Morimoto Y, Araki T, Uchida K, Tanaka K, Nakashima H, Hibi M, Kimura K, Inoue Y, Miki C, Kusunoki M. Intravital imaging of DSS-induced cecal mucosal damage in GFP-transgenic mice using two-photon microscopy. J Gastroenterol 2010; 45: 544-53.

[12] Koike Y, Tanaka K, Okugawa Y, Morimoto Y, Toiyama Y, Uchida K, Miki C, Mizoguchi A, Kusunoki M. In vivo real-time two-photon microscopic imaging of platelet aggregation induced by selective laser irradiation to the endothelium created in the beta-actin-green fluorescent protein transgenic mice. J Thromb Thrombolysis 2011; 32: 138-45.
[13] Morimoto Y, Tanaka K, Toiyama Y, Inoue Y, Araki T, Uchida K, Kimura K, Mizoguchi A, Kusunoki M. Intravital three-dimensional dynamic pathology of experimental colitis in living mice using two-photon laser scanning microscopy. J Gastrointest Surg 2011; 15: 1842-50.
[14] Tanaka K, Morimoto Y, Toiyama Y, Okugawa Y, Inoue Y, Uchida K, Kimura K, Mizoguchi A, Kusunoki M. Intravital dual-colored visualization of colorectal liver metastasis in living mice using two photon laser scanning microscopy. Microsc Res Tech 2012; 75: 307-15.
[15] Tanaka K, Morimoto Y, Toiyama Y, Matsushita K, Kawamura M, Koike Y, Okugawa Y, Inoue Y, Uchida K, Araki T, Mizoguchi A, Kusunoki M. In vivo time-course imaging of tumor angiogenesis in colorectal liver metastases in the same living mice using two-photon laser scanning microscopy. J Oncol 2012; 2012: 265487.
[16] Tanaka K, Okigami M, Toiyama Y, Morimoto Y, Matsushita K, Kawamura M, Hashimoto K, Saigusa S, Okugawa Y, Inoue Y, Uchida K, Araki T, Mohri Y, Mizoguchi A, Kusunoki M. In vivo real-time imaging of chemotherapy response on the liver metastatic tumor microenvironment using multiphoton microscopy. Oncol Rep 2012; 28: 1822-30.
[17] Tanaka K, Toiyama Y, Inoue Y, Uchida K, Araki T, Mohri Y, Mizoguchi A, Kusunoki M. Intravital imaging of gastrointestinal diseases in preclinical models using two-photon laser scanning microscopy. Surg Today 2013; 43: 123-9.
[18] Okabe M, Ikawa M, Kominami K, Nakanishi T, Nishimune Y. 'Green mice' as a source of ubiquitous green cells. FEBS Lett 1997; 407: 313-9
[19] Erpenbeck L, Schön MP. Deadly allies: the fatal interplay between platelets and metastasizing cancer cells. Blood 2010; 115: 3427-36.
[20] Gay LJ, Felding-Habermann B. Contribution of platelets to tumour metastasis. Nat Rev Cancer 2011; 11: 123-34.
[21] Buergy D, Wenz F, Groden C, Brockmann MA. Tumor-platelet interaction in solid tumors. Int J Cancer 2012; 130: 2747-60.
[22] Ubukata H, Motohashi G, Tabuchi T, Nagata H, Konishi S, Tabuchi T. Evaluations of interferon-γ/interleukin-4 ratio and neutrophil/lymphocyte ratio as prognostic indicators in gastric cancer patients. J Surg Oncol 2010; 102: 742-7.
[23] Liu H, Liu G, Bao Q, Sun W, Bao H, Bi L, Wen W, Liu Y, Wang Z, Yin X, Bai Y, Hu X. The baseline ratio of neutrophils to lymphocytes is associated with patient prognosis in rectal carcinoma. J Gastrointest Cancer 2010; 41: 116-20.
[24] Yu M, Stott S, Toner M, Maheswaran S, Haber DA. Circulating tumor cells: approaches to isolation and characterization. J Cell Biol 2011; 192: 373-82.
[25] Ghadially R. The role of stem and circulating cells in cancer metastasis. J Surg Oncol 2011; 103: 555-7.
[26] Huh SJ, Liang S, Sharma A, Dong C, Robertson GP. Transiently entrapped circulating tumor cells interact with neutrophils to facilitate lung metastasis development. Cancer Res 2010; 70: 6071-82.
[27] Spicer JD, McDonald B, Cools-Lartigue JJ, Chow SC, Giannias B, Kubes P, Ferri LE. Neutrophils promote liver metastasis via Mac-1-mediated interactions with circulating tumor cells. Cancer Res 2012; 72: 3919-27.
[28] Robertson JH, Sarkar S, Yang SY, Seifalian AM, Winslet MC. In vivo models for early development of colorectal liver metastasis. Int J Exp Pathol 2008; 89: 1-12.